Paper

Iron-Zircon Pigments Prepared by the Sol–Gel Method

Masashi SHOYAMA, Kyoko HASHIMOTO,* Tadanori HASHIMOTO,*
Hiroyuki NASU* and Kanichi KAMIYA*

Ceramics Laboratory of the Mie Prefectural Industrial Research Institute, 788, Higashiakuragawa, Yokkaichi-shi, Mie   510–0805
Department of Chemistry for Materials, Faculty of Engineering, Mie University, 1515, Kamihama-cho, Tsu-shi, Mie   514–8507

ゾル–ゲル法による Fe-$ZrSiO_4$ 顔料の合成

庄山昌志・橋本恭子*・橋本忠範*・那須弘行*・神谷寛一*

三重県工業技術総合研究所窯業センター，510–0805 四日市市東阿倉川 788
*三重大学工学部分子素材工学科，514–8507 津市上浜町 1515

The low temperature preparation of Fe-zircon pigment powders was conducted using the sol–gel method. The influence of firing atmosphere on the coloration and chemical durability of the pigment were examined, and the incorporation behavior of Fe ions into zircon matrix was discussed. The pigments were formed at lower temperature (900–1000°C) than that in the conventional solid-state method, when LiCl was added as a mineralizer (or catalyst) instead of conventional, the complicated mixture of several mineralizers. It was found that a large part of Fe ions is included in the pigment as α-Fe_2O_3. Fe-zircon pigments showed higher acid-durability compared to the commercial one, suggesting that α-Fe_2O_3 is embedded in the zircon matrix as uniformly distributed minute particles.   [Received December 2, 1998; Accepted March 26, 1999]

1. Introduction

Much of the progress in the knowledge of inorganic pigments over last two decades has been related with ceramic colors, because of the demand for high temperature colors for sanitary ware and for improved control of shade.[1]

Particularly, the development of new reddish inorganic pigments has been needed in the porcelain and sanitary industry, because, so far, the inorganic pigments of strong red color has been limited to Pb_3O_4 and CdS_xSe_{1-x}.[2],[3] Cadmium sulfoselenides are still an important current source of red color in ceramics.[4] But, they are not stable in glazes owing to high oxygen-sensitivity. In addition, in these days, it seems difficult for these conventional red inorganic pigments to clear the regulation shown in Table 1 for table wares due to the inclusion of poisonous elements such as Pb or Cd.[5]

Cr-alumina pink and Fe-zircon pink are other important candidates for the inorganic reddish color pigments. The chromium pigment shows a reflectance curve having double peaks, which is the origin of different shades of color under day light.[1] On the other hand, Fe-zircon pink shows a very regular reflectance curve.

In the case of the Fe-zircon pink pigment, the demand for high temperature colors for sanitary ware and for improved control of shade may be satisfied because of great stability of the zirconium silicate structure. The first commercial advertisement of an iron-zircon pink appeared in several

journals in 1960 from the Harshaw Chemical Co. as a "Persian Coral." Such a new high temperature pink stain having distinct advantages over the chromium pink was reported in the patent in 1961.[6]

However, production of Fe-zircon pigments through the solid-state reaction route requires high heat treatment temperature as above 1200°C, and also needs the complicated composite mineralizers which consist of NaF, NaCl and NH_4NO_3 or $NaNO_3$.[7] Furthermore, the formation of Fe-zircon pink is much more difficult to be controlled than that of other zircon pigments, and careful attention must be paid to the particle size of the zirconia used as a raw material and the silica-comminuting procedures must be carefully controlled.[8] Nevertheless, Fe-zircon pigment has become an important source of reddish color in ceramics, because it has great stability, non-poisonous property and superior reflectance property.

Sol–gel method is one of the important methods for the low temperature production of ceramics,[9]–[11] and may be also applicable to the preparation of Fe-zircon pigment. It has been reported that the coloration of the Fe-zircon pigment depends on its particle size; the color becomes lighter, redder and yellower as the particle size of pigment is reduced.[12] Therefore, the sol–gel method which enables us to make powders with desired size is considered to be favorable for the preparation of the Fe-zircon pigment. In addition, the incorporation of higher amount of Fe ions may be also expected in the sol–gel method than in the conventional method. In fact, other pigments including V-zircon blue pigment have been successfully synthesized by the sol–gel method, and the formation and coloration scheme have been studied in detail.[13],[14] The present authors have also succeeded in the preparation of rare-earth zircon pigments at temperatures below 1000°C using the sol–gel method.[15]

In the present study, the low temperature preparation of the Fe-zircon pigment powders by the sol–gel method was conducted. The influence of firing atmosphere on the coloration and the chemical durability of the pigments were examined, and incorporation behavior of Fe ions into zircon matrix was discussed.

Table 1. Permissible Limits for Lead and Cadmium Release for Ceramic Wares (ISO-6486)

Type of Ceramic Ware	n	Permissible Limit Criterion	Unit of measure	Pb Limit	Cd Limit
Flatware, fillable	6	Mean≦Limit	mg/l	3.0	0.50
Flatware, not fillable	6	Mean≦Limit	mg/dm²	1.0	0.13
Small Hollow-ware	6	All specimens≦Limit	mg/l	2.0	0.50
Large Hollow-ware	6	All specimens≦Limit	mg/l	1.0	0.25
Storage Hollow-ware	6	All specimens≦Limit	mg/l	0.5	0.25
Cups and Mugs	6	All specimens≦Limit	mg/l	0.5	0.25
Cooking Ware	6	All specimens≦Limit	mg/l	0.5	0.05

2. Experimental procedure

2.1 Preparation of samples

Table 2 shows the nominal compositions of the samples. In the table, x shows the molar ratio of Li and Fe to SiO_2, with the molar ratio of Li to Fe being kept at unity. Fe-zircon powders were prepared according to a flow chart shown in Fig. 1. Tetraethyl-ortho-silicate, $Si(OC_2H_5)_4$ (Wako Pure Chemical Ind., Ltd., TEOS) and zirconium oxychloride hydrate, $ZrOCl_2 \cdot 8H_2O$ (Wako Pure Chemical Ind., Ltd., ZOC) were used as raw materials for SiO_2 and ZrO_2, respectively. Since the hydrolysis rate of TEOS is low relative to ZOC, in order to attain intimate mixing of raw materials, TEOS was first partially hydrolyzed for 1 h at room temperature under acidic conditions with H_2O of $r=1.0$, where $r=[H_2O]/[TEOS]$ in molar ratio, and then hot ethanol solution (50°C) containing prescribed amount of ZOC and $FeCl_3 \cdot 6H_2O$ were added under stirring. LiCl was added to the solution at this stage as a mineralizing reagent. Gelation of the Li, Fe-containing ZrO_2-SiO_2 sol was achieved by adding an excess amount of water ($r=11$) at 80°C also under stirring. The resultant gel was dried at 100°C for 16 h in the air, followed by the heat-treatment at 700, 800, 900 and 1000°C in the air for 3 h. All the samples were also heat-treated at 1000°C under N_2 or O_2 atmosphere to examine the influence of firing atmosphere on the coloration of the Fe-zircon pigments.
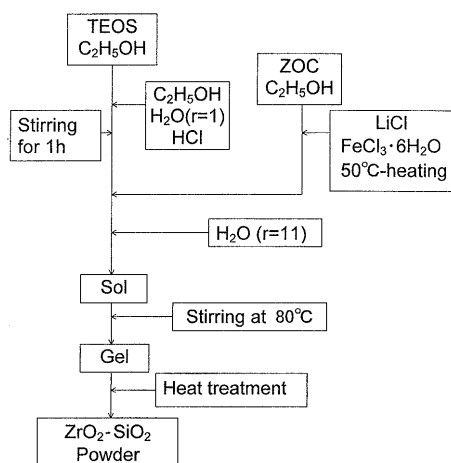

Fig. 1. Flow chart for the preparation of Fe-containing ZrO_2-SiO_2 gels.

2.2 Characterization of samples

The crystallization of the starting gels was followed by X-ray diffraction method using a Ni-filtered Cu Kα radiation (Shimadzu, XD-610). The fraction of zircon, α(ZR), in the heat-treated samples was determined by using X-ray diffraction (XRD) patterns. For that purpose, relative diffraction intensity of four lines appearing in the diffraction angle 2θ range from 26° to 32°, i.e., (200) line of $ZrSiO_4$, (111) and (11$\bar{1}$) lines of monoclinic zirconia (m-ZrO_2) and (101) line of tetragonal zirconia (t-ZrO_2), were used, and α(ZR) was estimated by the following equation.[16]

$$\alpha(ZR) = I_{ZR}(200)/(I_{ZR}(200) + I_M(111) + I_M(11\bar{1}) + I_T(101)),$$

where subscripts ZR, M and T stand for $ZrSiO_4$, m-ZrO_2 and t-ZrO_2, respectively, and numbers in the parentheses indicate the indicies of respective crystallographic planes. If any other crystalline species is co-precipitated, XRD intensity is involved in the denominator of the above equation.

Oxidation state of Fe ions in the heat-treated samples was examined on the basis of binding energy of Fe2p XPS line measured by using Mg Kα radiation with applied voltage of 8 kV (Shimadzu, ESCA750 and ESCA PAC 760). The binding energy was calibrated relative to C1s line at 284.6 eV.

The color parameters, CIE-$L^*a^*b^*$ and Munsell HVC value, were measured for obtained pigments with scanning spectrometer (Shimadzu, UV-3100 PC UV-NIR) using a CIE standard lighting C (color temperature: 6774 K) and visual field of 2°. In this system, L^* is color lightness ($L=0$ for black and $L=100$ for white), a^* is the green(−)-red(+) axis, and b^* is the blue(−)-yellow(+) axis. The color of the sample was estimated using the Munsell HVC value, according to JIS-Z-8102-1985.[17]

Chemical durability of the Fe-zircon pigment powders obtained at the heat treatment temperature of 1000°C (1000°C-treated pigment) was estimated by soaking the powders into 5% HCl solution for 15 min–168 h at room temperature. 1.0 g of the pigment powders was weighed and soaked in the 20-ml HCl solution at room temperature, followed by drying at 80°C. The amount of Fe ions dissolved into the soaking solution was determined by the atomic absorption spectrophotometer (Seiko Instruments, SAS7500).

The observations by scanning electron microscope (SEM; Hitachi, S-3200N) and line analysis of Si, Fe and Zr by electron dispersion X-ray analyzer (Horiba, EMAX-5770W) were made.

Table 2. Compositions of Starting Solutions (in the Molar Ratio)

Sample	Si TEOS	Zr $ZrOCl_2 \cdot 8H_2O$	C $FeCl_3 \cdot 6H_2O$	M LiCl	H_2O	HCl	C_2H_5OH
$x=0.3$	1	1	0.3	0.3	S:ZR=1:11 12	0.2	0.22
$x=0.1$	1	1	0.1	0.1	S:ZR=1:11 12	0.2	0.22
$x=0.05$	1	1	0.05	0.05	S:ZR=1:11 12	0.2	0.22
$x=0.01$	1	1	0.01	0.01	S:ZR=1:11 12	0.2	0.22

C:Chromophore, M:Mineralizer, S:SiO_2 ZR:ZrO_2,

3. Results

3.1 Formation of Fe-zircon pigments

Figure 2(a) shows the XRD patterns of the ZrO_2–SiO_2 gel samples with x of 0.3 which were heat-treated at different temperatures. At 600°C, t-ZrO_2 is a prevailing crystalline phase, and the gel starts to crystallize to form the zircon phase above 700°C. It is also seen that the fraction of zircon phase increases at the expense of t-ZrO_2 like in rare earth-containing ZrO_2–SiO_2 gels reported in the previous paper.[15] The similar trend of crystallization behavior was observed in the ZrO_2–SiO_2 gels with different x's. Crystalline species associated with Fe ions are scarcely observed in any XRD pattern in Fig. 2(a), but only in the 1000°C-treated sample a small XRD peak corresponding to α-Fe_2O_3 is detected in magnification shown in Fig. 2(b). Other Fe-containing crystalline compounds such as Fe_3O_4 and Fe_2SiO_4 were not observed in the sample.

Figure 3 shows the relationship between the fraction of zircon, $\alpha(ZR)$ and heat treatment temperature for the ZrO_2–SiO_2 gel containing Fe ions by 0.3 in x. The $\alpha(ZR)$ increases above 700°C, and reaches about 90% at 1000°C. The heat treatment temperature where zircon is formed is considerably lower than that required in the conventional solid-state reaction method.

Figure 4 shows the Fe and Li-content dependence of the fraction of zircon, $\alpha(ZR)$ and the fraction of ZrO_2 including monoclinic and tetragonal phases, $\alpha(mt)$ for the ZrO_2–SiO_2 gels heat-treated at 1000°C. It is seen that the $\alpha(ZR)$ drastically increases at $x=0.05$, with accompanying the decrease of ZrO_2 phase, and is almost saturated around

90% on further increase of the Fe and Li^+ ions.

3.2 XPS measurements of Fe ions

In Fig. 5, XPS spectrum of Fe ions in the 1000°C-treated sol–gel-derived Fe-zircon pigment with x of 0.3 is compared with those of α-Fe_2O_3 and FeS reagents as references of trivalent and divalent Fe ions, respectively. The XPS spectrum of Fe ions in the sol–gel-derived Fe-zircon pigment is very similar to that of α-Fe_2O_3 and is sited at a slightly higher binding energy value than divalent Fe ions (709.7
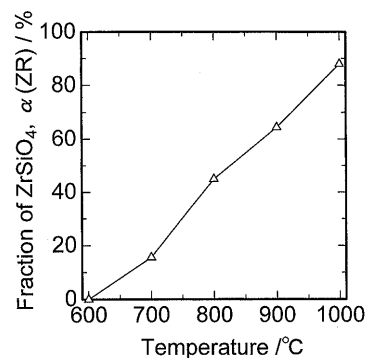

Fig. 3. Relationship between zircon fraction ($\alpha(ZR)$) and heat treatment temperature for the $(Li, Fe)_{0.3}$–ZrO_2–SiO_2 gel sample.

Fig. 4. Plots of the fraction of zircon, $\alpha(ZR)$, and ZrO_2, $\alpha(mt)$, as a function of (Li, Fe) molar ratio in $(Li, Fe)_x$–ZrO_2–SiO_2 gels.
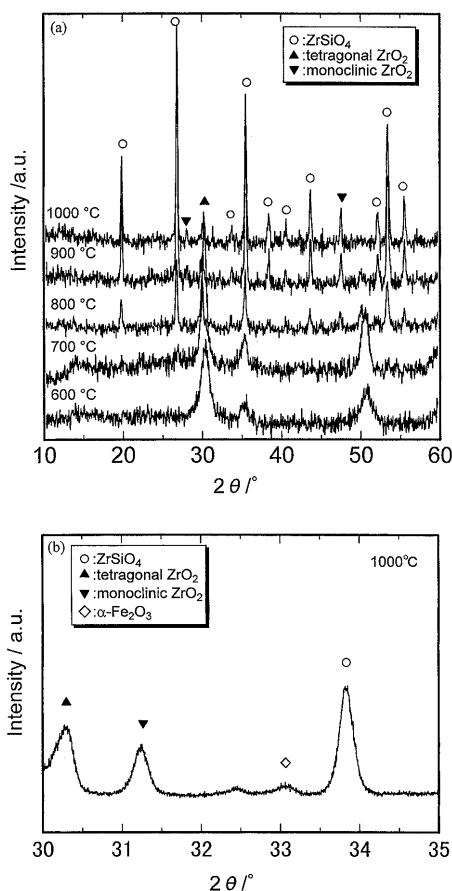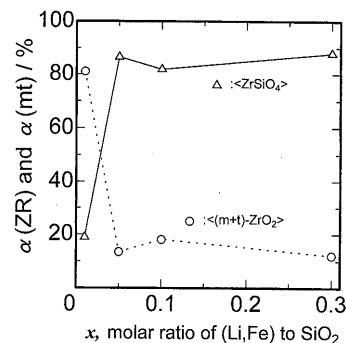

Fig. 2.(a) Change of XRD pattern of the $(Li, Fe)_{0.3}$–ZrO_2–SiO_2 gel with heat treatment temperature.
(b) Magnified XRD pattern of the $(Li, Fe)_{0.3}$–ZrO_2–SiO_2 prepared at 1000°C.

Fig. 5. XPS spectra of Fe2p of FeS, α-Fe_2O_3 and sol–gel-derived $(Li, Fe)_{0.3}$–ZrO_2–SiO_2 heat-treated at 1000°C.

eV), implying that the oxidation state of Fe ions in the pigment is mainly trivalent.

3.3 Chemical durability of Fe-zircon pigment

Figure 6 shows the soaking time dependence of the amount of Fe ions dissoluted from the 1000°C-treated sol-gel-derived Fe-zircon pigment into the 5% HCl solution at room temperature. For a comparison, results for commercial Fe-zircon pink pigment (M-66, Nitto Sangyo Co., Ltd.,
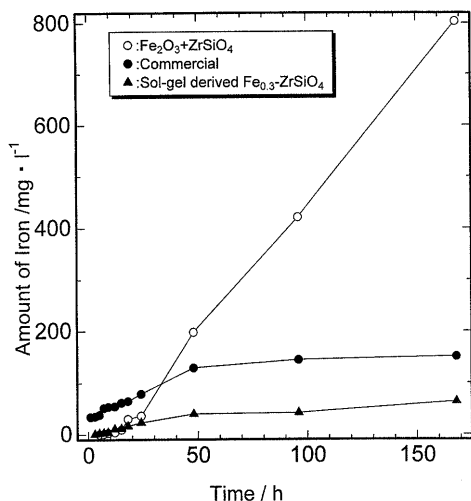

Fig. 6. Soaking time dependence of the Fe dissoluted from sol-gel-derived, commercial Fe-zircon pigments and powder mixture of $ZrSiO_4$ and α-Fe_2O_3.

Si : Zr : Fe = 1 : 0.86 : 0.05 in molar ratio) and the mixture consisting of $ZrSiO_4$ and α-Fe_2O_3 powders are also shown in the figure. The amount of dissoluted Fe ions increases with the soaking time in each sample. As is seen, the amount of dissoluted Fe ions for the sol–gel-derived Fe-zircon powder is about a half of the commercial one at any soaking time, although the content of Fe ions in the sol–gel-derived powder (Fe = 0.3 mol) is 6 times larger than the latter (Fe = 0.05 mol). In addition, Fe ions in the sol–gel-derived powder are dissolved 10 times slower than those in the powder mixture, though the content of included Fe ions is identical (Fe = 0.3 mol). This fact suggests that the surrounding of Fe ions in the sol–gel-derived pigment is different from those of Fe ions in the powder mixture, and even in the commercial pigment.

3.4 Color parameters

Table 3 shows the CIE-$L^*a^*b^*$ values, Munsell HVC values and color of the sol–gel-derived samples heat-treated at 900 and 1000°C. Figure 7 shows the Fe-content dependence of a^*-b^* value of the sol–gel-derived Fe-zircon pigment, where a^* and b^* mean CIE-$L^*a^*b^*$ values shown in Table 3. As the amount of added Fe ions increases, a^* value indicating the red component of the color moves from zero to the redder direction, approaching the value for the commercial pigment, and the samples with Fe ions of 0.1 in molar ratio become redder than commercial one. As the heat treatment temperature increases from 900 to 1000°C, b^* value indicating the yellow component slightly decreases.

Figure 8 shows the influence of acid test on the color of 1000°C-treated sol–gel-derived $Fe_{0.05}$-zircon pigment and the powder mixture of α-Fe_2O_3 and $ZrSiO_4$. After acid test,

Table 3. CIE-$L^*a^*b^*$, Munsell HVC Values and Color of the Sol–Gel-Derived Fe-Zircon Pigments Having the Composition of $(Li, Fe)_x$-ZrO_2–SiO_2 Heat-Treated at 900 and 1000°C

1000°C

Sample	L*	a*	b*	H	V	C	Color
x=0.01	78.6	1.1	18.8	1.4Y	7.7	2.7	Light grayish yellow
x=0.05	67.9	9.0	13.6	3.4YR	6.6	3.0	Light grayish orange
x=0.10	55.1	17.1	16.2	9.9R	5.3	4.6	Dull orange
x=0.30	42.0	11.2	12.9	2.5YR	4.1	2.9	Dark grayish orange

900°C

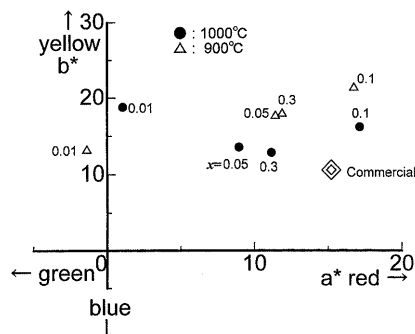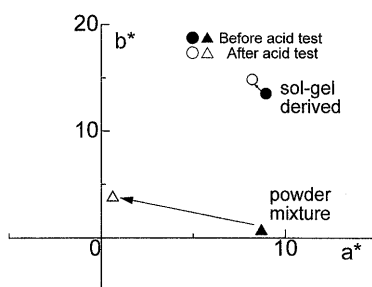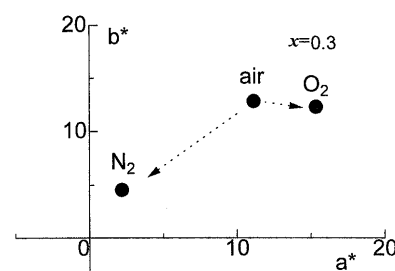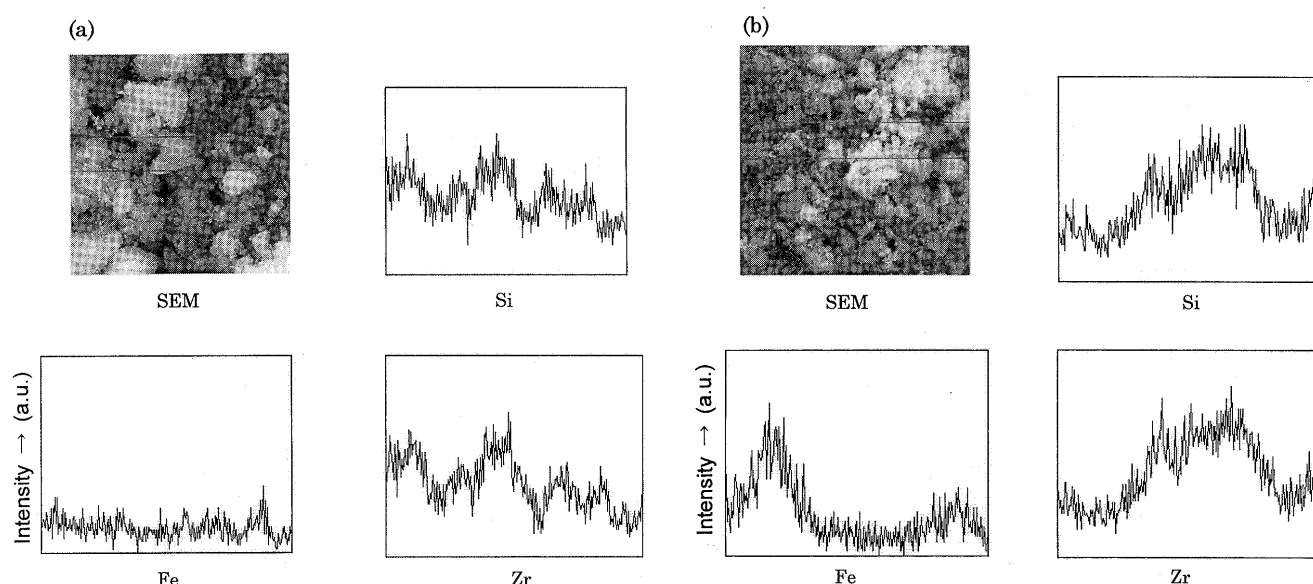| Sample	L*	a*	b*	H	V	C	Color
x=0.01	76.1	-1.4	13.1	4.3Y	7.5	1.7	Light yellowish gray
x=0.05	63.5	11.4	17.6	3.6YR	6.2	3.9	Grayish orange
x=0.10	55.6	16.7	21.3	2.4YR	5.4	5.0	Dull orange
x=0.30	45.4	11.9	18.0	4.2YR	4.4	3.7	Grayish orange
Commercial Fe-ZrSiO4	51.3	15.2	10.6	7.9R	5.0	3.8	Grayish red

Fig. 7

Fig. 8

Fig. 9

Fig. 7. a^*-b^* plots of the Fe-zircon pigment powders made using various chromophore concentration.
Fig. 8. Influences of acid-test on the color of the sol–gel-derived $Fe_{0.05}$-zircon pigment and powder mixture of α-Fe_2O_3 and $ZrSiO_4$.
Fig. 9. Influence of firing atmosphere on the color of the sol–gel-derived $Fe_{0.3}$-zircon pigment.

Table 4.   Volume Fraction of Crystalline Species in $(Li, Fe)_x$–$ZrSiO_4$ Gels Heat-Treated at $1000°C$ under Different Firing Atmospheres

Sample	$ZrSiO_4$/ %	$ZrO_2(m+t)$/ %	Hematite/ %	Magnetite/ %
$x=0.3$(in Air)	88.7	8.9	0.5	2.0
$x=0.3$(in O_2)	71.3	21.3	7.3	0
$x=0.3$(in N_2)	83.5	1.2	1.8	13.4

(a)

(b)

Fig. 10. (a)   SEM image and line analysis data of Si, Fe and Zr of the sol–gel-derived Fe-zircon pigment heat-treated at $1000°C$ $(x=0.3)$. (Analyzed area is between two lines in SEM image with $3 \mu m$ width).
(b) SEM image and line analysis data of Si, Fe and Zr of the powder mixture of α-Fe_2O_3 and $ZrSiO_4$ $(x=0.3)$. (Analyzed area is between two lines in SEM image with $3 \mu m$ width).

the de-coloration for sol–gel-derived Fe-zircon pigment was observed in a^* value, but only by 8%, while the decrease of a^* value was 97% for the powder mixture.

3.5 Influence of firing atmosphere

Table 4 shows the volume fraction of crystalline phases of sol–gel-derived Fe-zircon powders heat-treated at $1000°C$ under different firing atmospheres. The amount of hematite phase increases under O_2 atmosphere, while that of magnetite phase increases under N_2 atmosphere.

Figure 9 shows the color parameter changes of sol–gel-derived $Fe_{0.3}$-zircon powder heat-treated at $1000°C$ under different atmospheres. About 50% increase of red value (a^*) was observed in the case of O_2-firing, while serious color deterioration was caused by N_2-firing.

3.6 Scanning electron microscopy (SEM)

Figure 10(a) shows SEM image and results of line analyses of Si, Fe and Zr of the $1000°C$-treated sol–gel-derived Fe-zircon pigment powder with $x=0.3$, and in Fig. 10(b) results for the powder mixture of $ZrSiO_4$ and α-Fe_2O_3 with x of 0.3 are shown. In Fig. 10(a), the concentrations of Si and Zr fluctuate, corresponding to the distribution of discrete particles, while that of Fe shows almost no change through the analysis line area. As is seen in the Fig. 10(b), the distribution of Si and Zr elements in the powder mixture corresponds to the distribution of zircon particles as in the sol–gel-derived Fe-zircon pigment powder. But, Fe concentration in the powder mixture shows the distinct increase at α-Fe_2O_3 particles, naturally being due to the fact that α-Fe_2O_3 in the powder mixture is isolated from zircon particles.

4. Discussion

4.1 Low temperature formation of Fe-zircon pigments

Fe-zircon pigment was successfully prepared around $1000°C$, like the rare earth-containing zircon pigments was.[15] The temperature required for forming Fe-zircon pigments in the sol–gel method is relatively lower than that in the conventional solid-state reaction method. This fact may be ascribed to high reactivity and highly uniform mixing of raw materials in the starting sol and gel. However, even in the sol–gel method, the addition of a lithium compound as a mineralizer was indispensable to form Fe-zircon at such low temperatures. Regarding with the effect of mineralizer on the formation of zircon, several mechanisms have been proposed. Eppler[18] discussed the effect of halogens on the formation of zircon. Nurishi et al. observed the catalyzing or mineralizing effect of lithium compounds on the formation of zircon during the solid-state reaction below $1000°C$, although they proposed that the formation of zircon is essentially accelerated by the Hedvall effect, i.e., by the transformation of SiO_2 from quartz to cristobalite above $1000°C$.[19] On the contrary, present authors reported that the zircon formation in the ZrO_2–SiO_2 gels is mineralized by lithium compounds but is independent from anion species associated with Li^+ ions.[20] In addition, the facts, in the present and previous cases, zircon starts to be formed in the gels at $700°C$ and no crystalline SiO_2 is involved during the zircon formation indicate that the zircon formation may not be driven by Hedvall effect.

The heat treatment temperature dependence of the fraction of zircon formed in the gels was very similar to that of chromophore-free gels,[20] when LiCl was added as a mineralizer. Further, Fe ions did not exhibit any catalyzing effect by themselves on the zircon formation. Therefore, it is concluded that the species mineralizing zircon formation is not Fe ion but is Li^+ ion in the present case.

As for the role of Li^+ ions in the formation, the present

authors have tentatively proposed in the previous paper[20] that high-temperature form of Li_4SiO_4 metastably formed around 700°C may act as a seed for zircon, since any other Li-containing compounds such as $Li_2Si_2O_5$[19] was not observed to be formed.

Eventually, as described above, the advantages of the sol–gel method over the conventional solid-state method have also been exhibited in the preparation of Fe-zircon pigment powders. Namely, the pigment was prepared at relatively low heat treatment temperature with only one kind of mineralizer, instead of complicated mixture of several mineralizers used in the conventional method.

4.2 Chemical state of Fe ions in the sol–gel-derived Fe-zircon pigments

In the pigment samples heat-treated at 1000°C in the air, α-Fe_2O_3 (hematite) was confirmed from XRD pattern, and no other crystalline species such as Fe_3O_4 and Fe_2SiO_4 were not found (Fig. 2), which is consistent with XPS results showing that most of Fe ions in the pigments are trivalent. Further more, XRD peak intensity ratio of α-Fe_2O_3 to zircon in the 1000°C-treated sample with $x=0.3$ was close to that of the powder mixture of α-Fe_2O_3 and zircon with the same x. Consequently, it is considered that a large part of added Fe ions is present as α-Fe_2O_3 in the sol–gel-derived Fe-zircon pigments.

4.3 Color of the sol–gel-derived Fe-zircon pigments

The pigment obtained at 1000°C in the air showed the color change toward redder direction as the amount of Fe ions increased up to 0.1 in the molar ratio to SiO_2 or ZrO_2 as shown in Fig. 7. In addition, the coloration of the sol–gel-derived pigments showed almost no change after acid-test, while powder mixture of α-Fe_2O_3 and zircon changed in color to light yellowish gray. This little color change with the amount of Fe ions and by acid-test may be the reflection of molecular-scale mixing of chromophore ions and raw materials which should be attained during the sol-preparation.

Atmosphere during heat treatment also had a remarkable effect on the coloration and the fraction of hematite and magnetite for the 1000°C-treated pigment samples, as can be seen in Fig. 9 and Table 4. The increase of a^* value caused by firing under O_2 atmosphere may be due to the increase of volume fraction of α-Fe_2O_3. On the other hand, the decrease of a^* value when fired under N_2 atmosphere may be attributed the reduction of some part of Fe^{3+} ions to Fe^{2+} ions to form magnetite. These facts suggest that the presence of divalent Fe ions in the pigments is not favorable for the development of reddish color.

4.4 Distribution of α-Fe_2O_3 in the sol–gel-derived Fe-zircon pigments

Fe ions are found to be distributed uniformly over analyzed area in the 1000°C-treated sample as can be seen in Fig. 10(a). However, α-Fe_2O_3 particles, which have been revealed to be present by XRD, were too small to be observed in SEM micrographs. The distribution of α-Fe_2O_3 in the pigment is discussed in the following.

Figure 11 shows schematic illustrations of three possible types of distribution of α-Fe_2O_3 in the sol–gel-derived pigments. The model A is "inclusion type," where small discrete α-Fe_2O_3 particles are uniformly embedded in the zircon matrix. The model B is "covering type," where the zircon particles are covered with α-Fe_2O_3 thin layer, and model C is "grain boundary type," which corresponds to the mixture of α-Fe_2O_3 and zircon.

The results of acid-durability test of the sol–gel-derived pigments may tell us which model is most probable. As can be seen in Fig. 6, the amount Fe ions released from the sol-gel-derived pigment was about 1/10 of that from the mixture of α-Fe_2O_3 and zircon powders. Actually, the powder
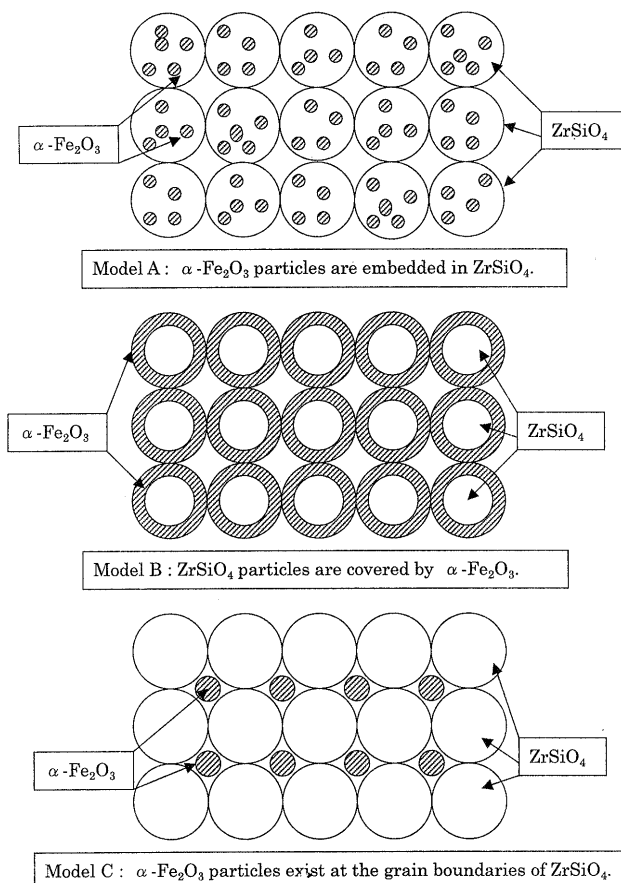

Fig. 11. Schematic presentation of possible models for the incorporation of Fe into $ZrSiO_4$ matrix.

mixture is almost colorless after leached for 168 h, while the sol–gel-derived pigment remains in red color. Such a large acid-durability is not expected in the models B and C because α-Fe_2O_3 is exposed to the acidic test-solution.

Eventually, it is considered that α-Fe_2O_3 is present in the zircon matrix as embedded minute particles so that it is highly protected from the environment.

5. Summary

The sol–gel method was applied to the preparation of Fe-zircon pigments. Following results were obtained.

(1) Fe-zircon pigment was successfully prepared by heat treating the gel made from $Si(OC_2H_5)_4$, $ZrOCl\cdot 8H_2O$ and $FeCl_3\cdot 6H_2O$ at 900–1000°C and by adding LiCl as a mineralizer. The preparation temperature was lower than that in the conventional solid-state method, and the pigment powders were obtained by simple process, namely without using complicated mixture of several mineralizers.

(2) The red color value and chemical durability of the pigments were improved, compared to the commercial pigment.

(3) The oxidation state of large part of Fe ions in the pigments was trivalent, and Fe^{3+} ions were considered to exist as minute α-Fe_2O_3 particles which are uniformly embedded in the zircon matrix.

References

1) R. W. Batchelor, *Trans. J. Br. Ceram. Soc.*, **73**, 297–301 (1974).
2) "Ganryo Binran," Seibun-do Shinko-Sha (1989) pp. 254–56 [in Japanese].
3) V. Lambies La Villa and J. M. Rincon Lopez, *Trans. J. Br.*

Ceram. Soc., **80**, 105–08 (1981).
4) A. C. Airely and W. Roberts, Ceram. Eng. Sci. Proc., Vol. 8 (1987) pp. 1168–75.
5) K. Kunieda and M. Shoyama, Mie Pref. Ceram. Res. Inst. Annual Rep., Vol. 28 (1993) p. 28 [in Japanese].
6) Brit. Pat., 986, 751.
7) U.S.Pat., 2, 166, 430.
8) Brit. Pat., 1, 227, 703.
9) K. Kamiya and T. Yoko, *Hyomen*, **15**, 131–42 (1986) [in Japanese].
10) K. Kamiya, S. Sakka and M. Mizutani, *J. Ceram. Soc. Japan* (*Yogyo-Kyokai-Shi*), **86**, 552–59 (1978) [in Japanese].
11) K. Kamiya, K. Takahashi, T. Maeda, H. Nasu and T. Yoko, *J. Eur. Ceram. Soc.*, **7**, 295–305 (1991).
12) C. Decker, *Am. Ceram. Soc. Bull.*, **71**, 296–300 (1992).
13) P. Tartaj, C. J. Serna and M. Ocana, *J. Am. Ceram. Soc.*, **78**, 1147–52 (1995).
14) G. Monros, J. Carda, M. A. Tena, P. Escribano, V. Cantavella and J. Alarcon, *Mater. Res. Bull.*, **27**, 753–60 (1992).
15) M. Shoyama, H. Nasu and K. Kamiya, *J. Ceram. Soc. Japan*, **106**, 279–84 (1998).
16) H. Kobayashi, T. Terasaki, T. Mori, H. Yamamura and T. Mitamura, *J. Ceram. Soc. Japan* (*Seramikkusu Ronbunshi*), **98**, 1109–13 (1990) [in Japanese].
17) Names of Non-Luminous Object Colors, JIS Z8102-1985.
18) R. A. Eppler, *J. Am. Ceram. Soc.*, **53**, 457–62 (1970).
19) Y. Nurishi, S. Nishimura, K. Takeuchi and T. Hibino, *Nihon-Kagaku-Zasshi*, **90**, 557–61 (1969) [in Japanese].
20) M. Shoyama, N. Matsumoto, H. Nasu and K. Kamiya, *J. Mater. Sci.*, **33**, 4821–26 (1998).